Numerical Simulation and Thermal Analysis of Pressurized Hydrogen Vehicle Cylinders: Impact of Geometry and Phase Change Materials

Mohamed-Amine Babay[1,*], Mustapha Adar[1], Souad Touairi[1], Ahmed Chebak[2], Mustapha Mabrouki[1]

[1] Laboratory of Industrial and Surface Engineering, Faculty of Science and Technologies, Sultan Moulay Slimane University, Beni Mellal, Morocco
[2] Green Tech Institute (GTI), Mohammed VI Polytechnic University, Benguerir, Morocco

ARTICLE INFO	ABSTRACT
    Keywords: 	This comprehensive study investigates the nuanced aspects of pressurized hydrogen vehicle cylinders during refueling, employing numerical simulation and thermal analysis. The examination encompasses the intricate dynamics influenced by cylinder geometry, mass flow rate variations, and the integration of phase change materials (PCMs). Simulations involving cylinders with diverse length-to-diameter ratios and inlet diameters highlight the impact of these parameters on temperature control. Notably, smaller length-to-diameter ratios prove effective for temperature regulation, while larger inlet diameters mitigate temperature rise. The study further explores the role of varying mass flow rates, revealing that an increasing flow rate during refueling results in the lowest temperature rise. In addition to geometry and mass flow rate considerations, the integration of PCMs is a focal point. Modeling and parametric analysis are employed to assess the feasibility of incorporating these materials. The study contributes valuable insights into optimizing the thermal performance and safety of hydrogen fuel systems. The holistic approach considers the interplay of geometry, mass flow rate dynamics, and the innovative use of PCMs, offering a multifaceted understanding of the factors influencing pressurized hydrogen vehicle cylinders.

1. Introduction

Hydrogen, recognized for its environmentally-friendly combustion byproducts, exceptional combustion efficiency, and renewable attributes, stands as a significant candidate for future secondary energy solutions [1,2]. It is anticipated that hydrogen will ultimately surpass fossil fuels and become the leading fuel choice for vehicles [3]. The increasing enthusiasm for hydrogen as a carbon-free fuel in the transportation sector stems from its ability to substantially decrease greenhouse gas emissions. Power-to-gas technology, which employs renewable energy sources for water electrolysis, offers an efficient approach to generate hydrogen for compact energy storage [4,5]. Unlike the complex battery systems used for electricity storage, hydrogen storage methods are

* Corresponding author.
E-mail address: mdamine.babay@gmail.com

simpler and do not entail the environmental consequences associated with the production of lithium-ion batteries and their associated greenhouse gas emissions [4,6].

The safe and efficient storage of hydrogen, particularly in the context of fuel cell vehicles, poses a crucial challenge for the transition to a low-carbon economy. One of the major issues is the control of heat transfer during the filling and emptying phases of high-pressure hydrogen tanks. This complex process involves three key components: convection between hydrogen and the inner wall, conduction through the wall, and convection between the outer wall and the air. The increase in gas temperature during filling presents significant challenges. Underlying reasons include the negative Joule-Thomson coefficient of hydrogen, kinetic energy transformed into internal energy, and compression due to the introduction of high-pressure gas. Mastering these elements is essential to avoid excessive temperatures that could compromise the safety and efficiency of the system. Hydrogen storage is a relatively understudied field, with limited research focusing on the use of phase change materials (PCMs) to manage heat generated during hydrogen fueling in metal hydride tanks, especially for stationary applications [7]. The exploration of PCMs as a solution to address heat-related challenges during the hydrogen fueling process has been a primary area of investigation in this research domain. The predominant method for onboard hydrogen storage involves the use of carbon fiber full-wrapped cylinders with either a metal or plastic liner, offering a high storage energy density. These gas cylinders with carbon fiber wrapping offer several advantages, including resistance to corrosion, extended lifespan, lightweight construction, exceptional strength, and a Leak Before Break (LBB) failure mechanism [8,9]. Consequently, the current emphasis in hydrogen storage research is centered around the utilization of carbon fiber cylinders for efficient and dependable onboard hydrogen storage, while investigations into PCM applications for hydrogen fueling are still in their early stages. To ensure an adequate operational range between refueling, hydrogen is stored at high pressures due to its low volumetric energy density at ambient conditions. Hydrogen tanks, whether they have a metal or plastic liner and glass fiber layers incorporate a carbon fiber outer shell to provide the necessary strength to withstand the storage pressures [10]. However, the use of CF shells imposes limitations on the amount of hydrogen that can be supplied to the tank during refueling. During the refueling process, compression of the gas inside the tank leads to an increase in temperature. If the temperature exceeds a certain threshold, it can cause damage to the CF liner, compromising the tank's structural integrity. To address this issue, the SAE TIR J2601 standard specifies that the gas temperature inside the tank should not exceed 85°C to prevent damage to the CF shell [11]. To maintain safe operating conditions and prevent damage to the carbon fiber (CF) shell, hydrogen is commonly pre-cooled to extremely low temperatures, reaching as low as -40°C. Although this pre-cooling step introduces complexities, increased costs, and an energy penalty to the refueling process, it is essential for ensuring that gas temperatures remain within safe limits and mitigating any potential risks to the CF shell.

Different methods have been explored for storing hydrogen, including compressed hydrogen, liquid hydrogen, metal hydrides [12,13]. Among these methods, high-pressure hydrogen storage has gained popularity due to its simplicity and cost-effectiveness. The preference for high-pressure storage is driven by its practicality and the existing infrastructure that supports it. Yang conducted thermodynamic analyses to explore the behavior of hydrogen as an ideal or non-ideal gas in storage tanks [14]. Mohamed and Paraschivoiu [15] conducted an inquiry into the influence of real gas behavior when hydrogen is discharged from a high-pressure chamber under adiabatic conditions. Dicken and Merida carried out both measurements and simulations aimed at comprehending temperature distribution inside a hydrogen cylinder throughout the refueling process. They considered various factors, including filling time and initial mass [16,17]. Liu *et al.,* [8] conducted research exploring the impact of mass filling rate, initial pressure, and ambient temperature on

temperature increases and distributions. Their investigations encompassed both experimental and numerical simulation methodologies [8]. Algorithms and operating ranges have been established by Pregassame *et al.,* [18], and Maus *et al.,* [19], to prevent overheating and over-pressure in hydrogen refueling stations. Zheng *et al.,* [1] proposed an optimized filling algorithm using a multi-objective optimization model to enhance utilization ratio and filling speed. Heitsch *et al.,* [9] investigated temperature distribution in cylinders considering liner materials and outer thermal insulation. Recent studies have aimed at understanding the temperature distribution during hydrogen tank filling by utilizing simulation approaches. Two primary methods have been employed in these studies: computational fluid dynamics (CFD) simulations using established tools and software packages, and reduced order thermal analysis [20-22]. CFD simulations offer detailed information on temperature, density, velocity distribution, and flow patterns inside the tank. However, they require significant computational resources and time. To address this, researchers have used simplified 2D geometries, although this may compromise the accurate representation of gravity and three-dimensional flow patterns. On the other hand, reduced order thermal analysis offers the advantage of requiring fewer computational resources. However, it relies on semi-empirical estimations of heat transfer coefficients and may have limitations in predicting heat transfer to the liner due to the lack of knowledge about the velocity distribution inside the tank. Despite these limitations, the reduced order thermal method enables the inclusion of various heat transfer modes and alternative liner materials in the model.

Zhao's *et al.,* [23] review aims to comprehensively analyze studies related to the emptying process of compressed hydrogen tanks. The scope appears to focus on understanding the dynamics, thermodynamics, and practical implications of hydrogen discharge from high-pressure storage vessels [23]. Liszka *et al.,* [24] primary objective is likely to develop and optimize a model for hydrogen fast fill processes, specifically focusing on cylinders lined with phase change material.

This study aims to explore innovative strategies to regulate temperature during refueling, focusing on two fundamental aspects. Firstly, the use of a thin layer of aluminum to confine phase change materials (PCMs) during melting, minimizing the impact on the total volume of the tank. Secondly, the structural design of the tank, composed of aluminum, epoxy-reinforced carbon fiber composites, and epoxy-reinforced fiberglass composites. This multilayer configuration aims to create a cylinder that is both lightweight and robust, capable of withstanding the high pressures inherent in hydrogen storage for mobile applications, including vehicles. By incorporating PCMs and optimizing the multilayer design, this study seeks to establish a solid foundation for more efficient thermal management of hydrogen tanks. The results of this research could potentially inform future technological advancements in the field of hydrogen storage, thereby contributing to the realization of a more sustainable and environmentally friendly energy infrastructure.

2. PCMs for Hydrogen Storage

This study focuses on categorizing phase change materials (PCMs) based on factors like intended use, melting temperature range, chemical composition, latent heat, and cost, with paraffins, hydrated salts, organic compounds, and inorganic compounds being potential candidates [25]. The selection depends on measured thermophysical properties such as thermal conductivity, density, melting temperature, and heat of fusion. For hydrogen gas storage applications, optimal PCMs should exhibit high latent heat and conductivity in both solid and liquid phases, along with low density. The melting temperature should fall within the practical operating range of 52°C to 68°C to prevent spontaneous melting in hot climates. Considerations include health risks, flammability, physical hazards, and cost-effectiveness. Paraffin waxes, known for stability, chemical inertness, and non-

toxicity, are identified as suitable for hydrogen storage tanks due to advantageous melting temperatures and moderate latent heats. Commercial-grade paraffins, cost-effective blends derived from petroleum distillation, are preferred. Despite their advantages, limitations exist, particularly in thermal conductivity. Various methods, like incorporating metallic fillers and using metal or graphite matrix structures, aim to enhance thermal conductivity. A high-porosity graphite matrix with 95wt% paraffin shows promise in significantly improving effective thermal conductivity [26]. As shown in Table 1, while no single material possesses all desired characteristics, paraffin wax stands out due to favorable properties and ongoing research efforts to enhance its thermal conductivity. In this study, paraffin wax is selected as the most promising candidate for simulations addressing heat absorption during hydrogen fueling in storage tanks.

Table 1
Potential Phase Change Materials and their Property

Compound	Melting T	Heat of fusion	Conductivity	Density
Paraffin wax [27,28]	65 ∘C	173.6 kJ/kg	0.167 (liquid at 63.5 ∘C) W/m.K	790 (liquid at 65 ∘C) kg/m^3
C_{13-24} [29]	22-24 ∘C	189 kJ/kg	0.20 (solid) W/m.K	760 (liquid at 70 ∘C) kg/m^3
C_{23-45} [29]	58-60 ∘C	188 kJ/kg	0.20 (solid) W/m.K	795 (liquid at 70 ∘C) kg/m^3

3. Theoretical Examination

3.1 Development of a Thermodynamic Model and Exploration of Temperature Elevation Factors

During the gas filling process, temperature elevation results from various factors, including the negative Joule–Thomson coefficient during isentropic expansion, gas energy conversion within the cylinder, and gas compression. Despite the temperature increase, this effect is partially counteracted by heat transfer from hydrogen. The rapid filling of hydrogen introduces additional elements such as the Joule-Thomson effect, kinetic to internal energy conversion, and gas compression, all contributing to the overall temperature rise. To mitigate this temperature increase, a heat transfer process is employed, dissipating some heat to the surroundings while storing some within the cylinder material. To simplify the computational fluid dynamics (CFD) model for the intricate refueling process, several key assumptions are introduced, aiming to streamline the complexity of the simulation. Initially, we assume that, at the commencement of the refueling process, both the stationary hydrogen tank and the vehicle cylinder share the ambient temperature. This assumption is grounded in the significant prior heat exchange between the components. The establishment of natural convection at the outer cylinder wall is considered, incorporating a consistent convective heat transfer coefficient to account for heat dissipation. Additionally, to further simplify the model, we disregard energy exchange between hydrogen and the pipeline, a simplification justified by the high gas velocity during the refueling process. This simplifying assumption allows us to focus on the core dynamics without introducing unnecessary complexities.

Furthermore, we assume that the pressure at the cylinder inlet is equal to that in the stationary tank. This assumption is made under the condition of experimental simulations and is set at a value of 34 MPa. This assumption ensures a consistent pressure boundary condition for the numerical simulations. Considering the negligible impact of gravity effects for mass flow rates surpassing 0.02 kg/s during refueling, the model adopts an assumption of axisymmetry within the vehicle cylinder. This choice simplifies the geometry representation, leading to a 2-dimensional axisymmetric model for numerical simulations. By assuming axisymmetry, we reduce the computational complexity while capturing the essential features of the refueling process. In summary, these assumptions collectively aim to simplify the CFD model, making it more computationally manageable while retaining the essential dynamics of the refueling process. Figure 1 further enhances our understanding by

providing a visualization of the cylinder wall's structure and thermodynamic model. The heat transfer between hydrogen and the surrounding environment involves three distinct components. Convective heat transfer primarily occurs between the pressurized hydrogen and the inner cylinder wall. Subsequently, heat conduction takes place within the cylinder wall structure, followed by convective heat transfer between the outer surface of the cylinder and the surrounding air. These integral components collectively constitute the entire heat exchange process during refueling. For a comprehensive understanding of the cylinder's construction, Table 3 offers a detailed overview of the material properties inherent to each laminate comprising the cylinder wall. This data contributes to an enhanced understanding of the unique attributes and behaviors exhibited by each layer.

3.2 Factors Contributing to Temperature Elevation

During fast filling, when disregarding heat transfer to the surroundings, Liu *et al.,* [8] defined the final temperature using the real gas equation as follows

$$T_2 = \frac{\lambda \mu T_1 (T_1 + \alpha P_1) - \alpha(\lambda P_1 T_1 - P_1 T_1)}{T_1 + \alpha P_1 + \frac{\alpha T_1 P_1 - T_1 P_1}{P_2}} \tag{1}$$

The final temperature in an adiabatic filling process can be calculated employing Eq. (1), where we define λ as C_{P_0}/C_{V_2} and $\mu = C_{V_1}/C_{V_2}$. Utilizing data from Dicken and Mérida [16], we assume values of λ and μ to be 1.39 and 0.971, respectively. Both experimental and simulated data underscore the key drivers of temperature elevation during refueling as the mass filling rate, ambient temperature and initial pressure [16]. Remarkably, our study reveals distinct trends in temperature increase. Specifically, we observe an exponential relationship between temperature rise and mass filling rate, indicating a nonlinear connection. Additionally, we find that the relationship between temperature escalation and initial pressure or initial temperature follows a linear pattern within our experimental setup [16]. Upon analysis, the maximum temperature rises during refueling (T_{rise}) can be expressed using the following equation

$$T_{rise} = a \cdot b^{V_{mass}} + 0.3\,T_1 - 2.2P_1 + f \tag{2}$$

In this context, (T_{rise}) is measured in degrees Celsius, (V_{mass}) signifies the mass filling rate in g/s, (T_1) represents the ambient temperature in degrees Celsius, and (P_1) is the initial pressure of hydrogen within the cylinder in MPa. (a), (b), and (f) are obtained through numerical fitting, and their substitution results in the simplified equation

$$T_{rise} = -68.1 \times 0.9^{V_{mass}} + 0.3\,T_1 - 2.2P_1 + 68 \tag{3}$$

For refueling processes concluding with a final pressure below 34 MPa, an adjustment coefficient (C_T) corrects Eq. (3), and its association with the final pressure (P_2) is expressed as:

$$C_T = 1.01 - 1.52e^{-P_2/8.44} \tag{4}$$

If the final pressure does not surpass 34 MPa, the empirical formula for determining the maximum temperature rise is expressed as

$$T_{rise} = C_T(-68.1 \times 0.9^{V_{mass}} + 0.3T_1 - 2.2P_1 + 68) \tag{5}$$

These findings align with the work of Zhao *et al.,* [30], who have conducted a comprehensive investigation through a combination of experimental and simulation methods. Their research not only confirms the equivalence of initial temperature and ambient temperature but also establishes a valuable empirical formula that encapsulates these temperature dynamics. This empirical formula is instrumental in comprehending the intricate interplay between temperature, mass filling rate, and initial conditions in our study. It is crucial to highlight that the initial pressure falls within the range of 2 MPa to 34 MPa, during which Eq. (2), Eq. (3) and Eq. (5) are deemed accurate with minimal error. In real refueling scenarios, variations in the initial temperature within the cylinder and the material temperature from the ambient temperature may occur. In this context, (T_1) in Eq. (2), Eq. (3) and Eq. (5) denotes the higher of these temperatures, ensuring a conservative prediction for enhanced safety. Eq. (5) furnishes a convenient approach for computing the maximum temperature rise and, consequently, the maximum temperature during refueling. Adjusting the mass filling rate appropriately allows for control over the maximum temperature.

3.3 Theoretical Analysis on Temperature Rise

Formulated based on the underlying assumptions, the CFD model is constructed, taking into account factors such as heat transfer, turbulence, and real gas properties. Utilizing Reynolds averaging techniques within this model, we outline the specific governing equations, beginning with the mass conservation equation:

$$\frac{\partial \rho}{\partial t} + \frac{\partial}{\partial x_i}(\rho u_i) = 0 \tag{6}$$

In the given equations, where (ρ) stands for density, (t) denotes time, (u) represents the velocity tensor, and (x) indicates distance. The equation that embodies the fundamental principle of the first law of thermodynamics as applied to open systems is a crucial reference in our work. It can be located in the cited sources [8,31]

$$dU = dHin_{in} - dH_{out} + \delta Q - \delta W \tag{7}$$

δQ the work performed by the system (kJ).

$$dU = dH_{in} + \delta Q \tag{8}$$

The ultimate energy is denoted as

$$U_2 = U_1 + dU \tag{9}$$

$$U_2 = U_1 + dH_{in} + \delta Q \tag{10}$$

In our research, we delve into the relationship that links the specific internal energy of hydrogen with temperature is represented in Eq. (11). This intricate correlation plays a pivotal role in understanding the thermodynamic behavior of hydrogen within our study. We have detailed this correlation extensively to shed light on how specific internal energy varies with changes in temperature. By examining this relationship, we aim to uncover valuable insights into the energy dynamics of hydrogen, which is fundamental to our investigation. where u is specific internal energy, [kJ/k]. Parameters y and z are coefficients that correlate with temperature and specific internal

energy. As per data from Dicken and Mérida [16], the values for y and z are assumed to be 10.52 and 482.45, respectively.

$$u = y\,T - z \tag{11}$$

$$U_1 = m_1(yT_1 - z)\,;\ U_2 = m_2(y\,T_2 - z) \tag{12}$$

m_1 , m_2 (kg) initial or final mass of hydrogen within the cylinder. The ultimate mass:

$$m_2 = m_1 + \int \dot{m}dt \tag{13}$$

The enthalpy introduced into the system

$$dH_{in} = h_{in} \int \dot{m}dt\,;\ \delta Q = \int q dt \tag{14}$$

The ultimate temperature can be derived from the simultaneous equations provided as

$$T_2 = \frac{m_1(yT_1 - z) + h_{in}\int \dot{m}dt + \int q dt}{y(m_1 + \int \dot{m}dt)} - \frac{z}{y} \tag{15}$$

4. Modeling and Simulation
4.1 Hydrogen Cylinder Configuration

The illustration of the hydrogen vehicle cylinder's structure is presented in Figure 1. For a more comprehensive understanding, the cylinder wall (1) comprises three layers: an aluminum liner, a carbon fiber/epoxy, and a glass fiber-epoxy, as shown in Figure 1, depicting the design of the 34 MPa, 120 L cylinder. Key simulation dimensions can be found in Figure 1, while the second type of cylinder features an aluminum lining and includes phase change materials in Figure 2. Specific dimensions for various cylinders used in the simulations are detailed in Table 2, and Table 3 provides comprehensive information on the wall's material properties [30]. Table 2 provides detailed dimensions for various cylinders utilized in the simulations. Additionally, the material properties of the cylinder wall can be found in Table 3.
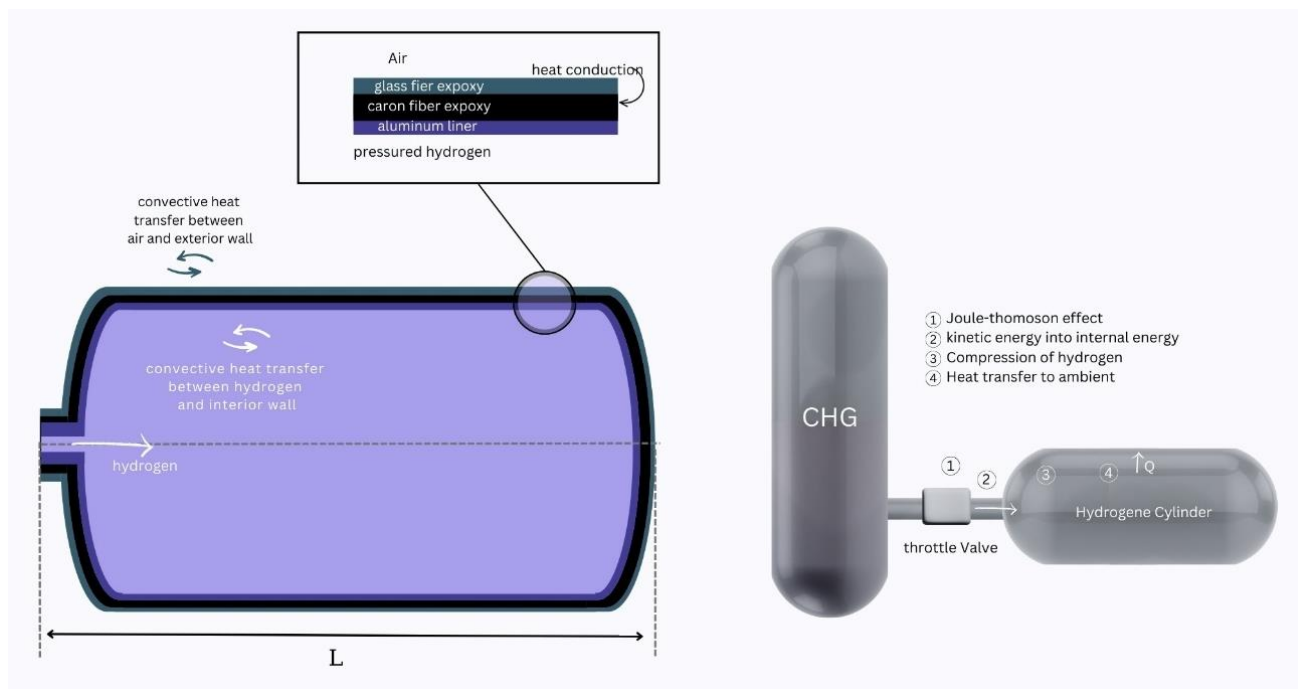
Fig. 1. Integrated Structure, Thermodynamic Model, and Schematic Representation of the Refueling Process for a Hydrogen Cylinder
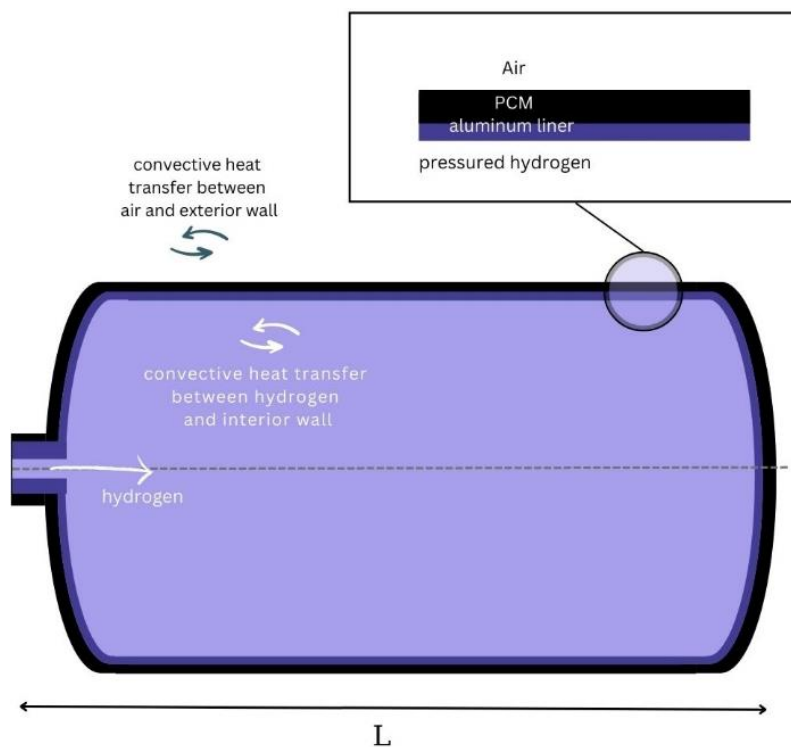
Fig. 2. Hydrogen Cylinder an aluminum lining and includes phase change materials

Table 2
Dimensions of the tank

Description	Dimensions (m)
Length of tank	1.025
Inner diameter of tank	0.404
Outer diameter of tank	0.434
Thickness of AL liner	0.004
Thickness of Carbo fiber	0.010
Thickness of glass fiber	0.001
Length of tube protruding into tank	0.08
Inner dimeter of inlet tube	0.006
Thickness of tube wall	0.004

Table 3
Material Characteristics for Each Tank Wall Laminate

| Laminate	Density	Specific heat	Thermal conductivity
Aluminum liner	2702 (kg/m^3)	900 (J/kg.K)	236 (W/m.K)
Carbon fiber epoxy	1515 (kg/m^3)	922 (J/kg.K)	3.74 (W/m.K)
Glass fiber epoxy	2052 (kg/m^3)	879 (J/kg.K)	0.14(W/m.K)

4.2 Model Assumptions

The simulation strategy employed the standard $k - \varepsilon$ turbulence model, a widely-used approach for modeling turbulence in fluid dynamics. This model relies on two crucial parameters: turbulence kinetic energy (k) and the rate of turbulent energy dissipation (ε). These parameters play a pivotal role in characterizing the complex flow patterns and turbulence within the hydrogen vehicle cylinder during the refueling process. The specific constants utilized in the $k - \varepsilon$ model was carefully selected to ensure the accuracy and reliability of the simulation results. These constants, denoted as $C_{1\varepsilon}$, $C_{2\varepsilon}$, $C_{1\mu}$, σ_k, and σ_ε , were set at 1.44, 1.92, 0.09, 1.0, and 1.3, respectively. These values are crucial in determining the behavior of turbulence within the computational domain. To execute these simulations, the Fluent 2021 R1 CFD software was chosen for its robust capabilities in handling complex fluid dynamics scenarios. The selection of a two-dimensional axisymmetric swirl CFD model was driven by the need to accurately capture the symmetric swirl structure inherent in the refueling process. This modeling choice is vital for obtaining a detailed understanding of how the hydrogen gas interacts with the internal surfaces of the cylinder. To represent the real gas properties of hydrogen, a Redlich-Kwong-based real gas model was adopted. This choice ensures that the simulation accounts for the compressibility and non-ideal behavior of hydrogen under the high-pressure conditions characteristic of refueling processes. It is essential for a realistic depiction of the thermodynamic properties of hydrogen within the cylinder. The Redlich-Kwong equation of state is a mathematical model that describes the behavior of real gases, particularly their deviation from ideal gas behavior. It was proposed by chemists Otto Redlich. The equation is expressed as follows

$$P = \frac{RT}{V-b} - \frac{a}{V(V+b)} \tag{16}$$

P is the pressure of the gas,
T is the temperature,
V is the molar volume,
R is the ideal gas constant,
a and b are constants specific to the gas.

The Redlich-Kwong equation offers improved accuracy over the ideal gas law by considering the attractive and repulsive forces between gas molecules. However, it still has limitations and may not be suitable for all gases and conditions. The Redlich-Kwong equation of state (RK EOS) is a thermodynamic model that describes the behavior of real gases. It takes into account the attractive and repulsive forces between gas molecules, providing a more accurate representation compared to the ideal gas law. However, the equation itself does not explicitly consider the effects of hydrogen storage cylinders. In the context of hydrogen storage, the RK EOS can be employed to model the thermodynamic properties of hydrogen gas under various conditions, such as different temperatures and pressures. The equation helps predict how hydrogen behaves within the storage cylinder, considering factors like compression and temperature changes. To account for the influence of hydrogen storage cylinders, additional considerations related to the cylinder material, geometry, and heat transfer characteristics would need to be incorporated. For a comprehensive analysis, one might couple the RK EOS with heat transfer equations and cylinder material properties to model the complete behavior of the hydrogen storage system, including the impact of the storage cylinder on the thermodynamics of the stored hydrogen gas. The meshing strategy, a critical aspect of CFD simulations, involved a structured quad grid for both the gas region and the walls. The mesh size was carefully tailored to different regions of the cylinder, considering factors such as gas flow rates and the need for computational accuracy. For the simulations involving the phase change material (PCM), the mesh consisted of 20409 nodes and 17479 elements. Conversely, for the cylinder without PCM, the mesh comprised 19183 nodes and 16432 elements showed in Figure 3. The mesh size in the cylinder's internal region was set at 4 mm × 4 mm, optimized for capturing detailed flow phenomena. In contrast, the inlet, where gas flow rates are higher, featured a more refined mesh size of 2 mm × 4 mm. The wall mesh size, set at 1 mm × 4 mm, was specifically chosen to ensure a sufficient number of computational nodes for accurate predictions of heat transfer and temperature distribution. In terms of temporal considerations, a time step size of 0.05 s was selected for all simulations. This temporal resolution allows for capturing dynamic changes in the system with sufficient detail. Additionally, a maximum of 20 iterations per time step was employed to strike a balance between computational efficiency and accuracy. Manual control mechanisms were integrated into the simulation process to cease iterations when the final pressure within the cylinder reached the predetermined threshold of 34 MPa. Overall, the simulation approach and modeling choices were tailored to strike a delicate balance between computational efficiency and accuracy, ensuring a realistic representation of the complex fluid dynamics and heat transfer phenomena within the hydrogen vehicle cylinder during refueling.
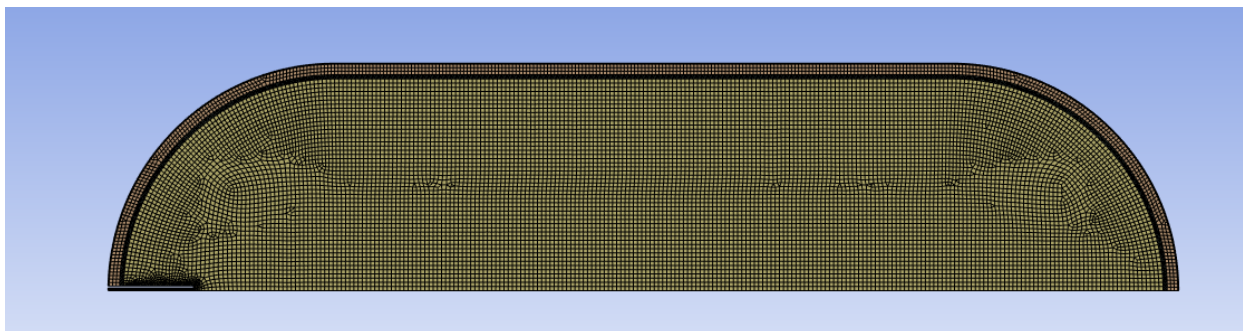
Fig. 3. Mesh used for the validation of the CFD model

4.3 Boundary and Initial Conditions Assessment

The numerical simulation involves specific initial and boundary conditions, which are comprehensively outlined in Table 4. We have set the inlet mass flow rate to 16 g/s. These configurations are based on the assumption that ambient temperature, gas inlet temperature, and initial gas temperature are all maintained at room temperature, precisely 293.2 K. Additionally, we've defined the initial and final pressures as 2 MPa and 34 MPa, respectively. To account for heat transfer between the tank outer surface and the surrounding air, a convective heat transfer coefficient of 10 W/m²·K has been employed.

Table 4
Boundary and initial conditions

	Value
Convective heat transfer coefficient from the outer surface of the cylinder to the surrounding ambient air	$10 \text{ W/m}^2 \text{ K}$
Inlet mass flow rate hydrogen	0.016 kg/s
Gas inlet temperature	293 K
Initial gas pressure	2 MPa
Initial gas temperature	293 K
Ambient temperature	293 K
Final gas pressure	34 Pa

5. Results and Discussions

5.1 Validation of Simulation Results

Liu *et al.,* [8] introduced a theoretical approach (Eq. (1)) to predict the final temperature, while Zhao *et al.,* [30] developed a fitting formula (Eq. (5)) based on their simulation findings. In our study, we focused on simulating Cylinder (1) to generate a final temperature curve. Figure 4 illustrates the final temperature curves derived from Liu *et al.,*'s [8] theoretical calculation, and showcases Zhao *et al.,*'s [30] fitting formula, along with our own calculation and simulation results. Both Eq. (1) and Eq. (2) relate the final temperature to the final pressure, while we introduced Eq. (13) to characterize the final temperature in relation to flow time. The specific final pressure values we utilized were obtained from our simulation results. By incorporating these final pressure values into Eq. (1) and Eq. (2), we constructed a final temperature curve as a function of time, as shown in Figure 4. In Eq. (15), we established a connection between the final temperature and flow time, assuming a constant parameter q. For the initial condition, we adopted a value of h_{in} = 4116.4 kJ/kg, guided by data from Dicken and Mérida [16]. Figure 4 highlights that Liu *et al.,*'s [8] theoretical calculation yields a slightly higher curve than the others, mainly because it doesn't consider heat transfer to the ambient environment. Additionally, there's a noticeable deviation between the calculated and simulated results for flow times less than 50 s. This discrepancy arises from the dynamic nature of heat transfer during the refueling process.
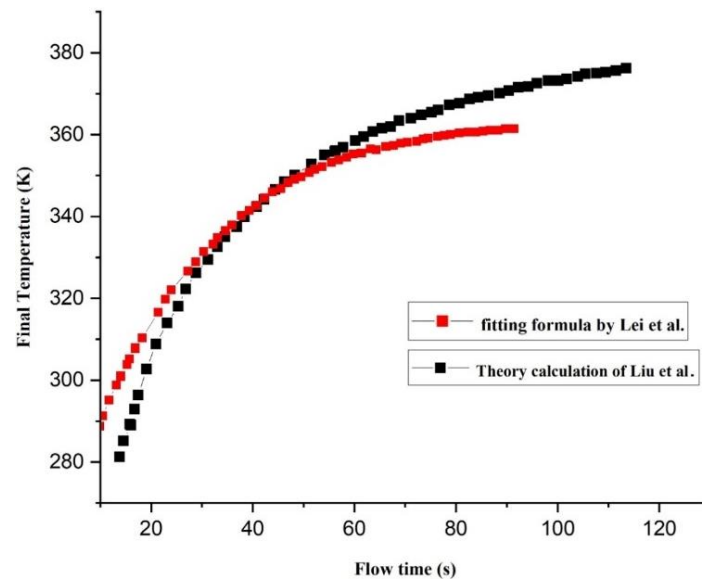
Fig. 4. Liu's Theoretical Calculation of Final Temperature and Final temperature of the fitting formula of Zhao *et al.,* [30]

5.2 Assessing the Impact of Length-to-Diameter Ratios

To investigate the influence of different length-to-diameter ratios, we conducted numerical simulations with two specific ratios, namely $l_\mathrm{a}: D_a = 3.4$ and $l_\mathrm{a}: D_a = 2$. The resulting trends in maximum and mean temperatures at various time intervals for these ratios are illustrated in Figure 5. It is evident from the graph that the maximum temperature within the cylinder consistently exceeds the mean temperature during the entire refueling process. Notably, the mean temperature of the hydrogen within the cylinder exhibits an exponential relationship with flow time for both cylinders. Intriguingly, within cylinder A, the maximum temperature is not observed at the conclusion of the refueling process but rather occurs at t=30 seconds. As time progresses, the temperature gradually increases to reach its peak before subsequently decreasing. Conversely, within cylinder B, the maximum temperature is achieved precisely at the end of refueling. The temperature profile in this case includes an initial increase, followed by a decrease, before ultimately reaching the maximum temperature. This observation provides valuable insights into the dynamic temperature behavior within these cylinders under varying length-to-diameter ratios. The selection of an appropriate ratio of length to diameter is crucial for effectively controlling temperature rise and distribution. A smaller ratio of length to diameter can facilitate temperature control. However, it's important to consider that a smaller ratio results in higher hoop stress, necessitating a thicker cylinder wall. This, in turn, increases the cost and reduces the gravimetric density of the cylinder. Achieving optimal temperature control while balancing structural considerations and vehicle limitations is a key aspect in the design and optimization of hydrogen storage systems. Further research can delve into exploring innovative approaches to enhance temperature management and overall system performance.
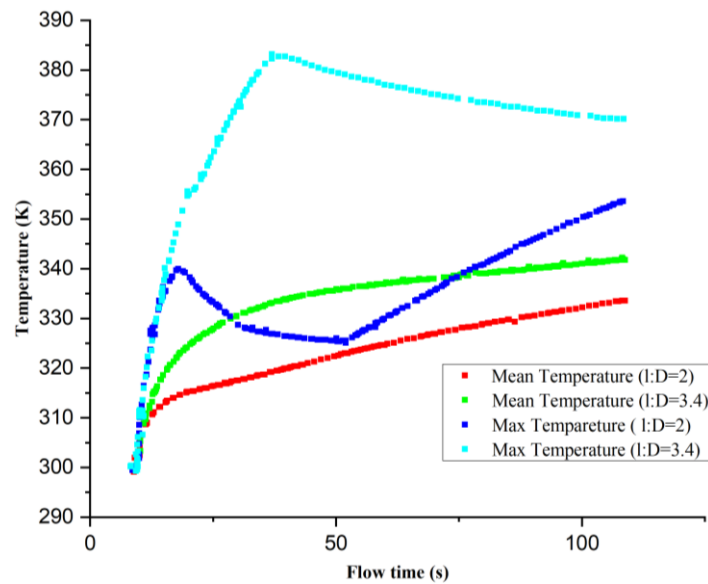
Fig. 5. Assessing Maximum and Average Temperatures in the Course of Refueling with Different Length-to-Diameter Ratios

5.3 Temperature Distribution During Refueling

Figure 6 provides a visual representation of the temperature distribution across the cylinder standard interfaces. An important observation is the relatively minor temperature difference between the H_2-Al and Al-Carbon interfaces. This phenomenon can be attributed to the aluminum liner's superior specific heat capacity and thermal conductivity when compared to the other materials involved. Furthermore, it's worth noting that the temperature at the Al-C interface surpasses that of the Carbon-Glass interface, which, in turn, is higher than the temperature at the Glass-Air interface. This temperature variation pattern across the interfaces offers valuable insights into the heat transfer dynamics within the cylinder, primarily driven by the distinct thermal properties of the materials involved. In the cylinder, the maximum temperature point is typically located near the bottom. This behavior is influenced by the specific gas flow dynamics within the cylinder. The temperature distribution is intricately linked to the flow patterns of the hydrogen gas in the system. Notably, the maximum temperature tends to appear in the recirculation region, as shown in Figure 7. In Figure 6, the temperature distribution along the axis and each interface of the cylinder wall at t = 50 s is depicted, providing valuable insights into the thermal behavior during the refueling process. The gas temperature along the axis experiences a rapid increase in the axial direction, peaking at 345.15 K (72 °C) when X = 1.1 m. This temperature then decreases swiftly with the increasing axial position (X). The observed temperature trends reveal the dynamic nature of heat transfer within the cylinder. The variations in temperature magnitude are closely tied to the specific laminate used in the cylinder construction. Notably, forced convection heat transfer plays a pivotal role in shaping the temperature distribution. At the interface between the aluminum liner and hydrogen gas, a substantial temperature rise is evident, reaching a maximum value of 344 K (70 °C). This significant temperature increase has implications for the aluminum liner, indicating a rapid heating process due to the interaction with the compressed hydrogen gas. Figure 6 further highlights the differential temperature rise at the interfaces, particularly between the aluminum liner and the carbon fiber/epoxy compared to the interface between the carbon fiber/epoxy and the glass fiber/epoxy. The higher heat transfer coefficient on Al-C contributes to a more pronounced temperature increase, underlining the importance of material selection in influencing thermal performance. The outer wall

experiences minimal heat transfer, attributed to the low thermal conductivity of the glass fiber/epoxy composite. Despite this, the interaction with convection between the outer wall and the environment leads to a gradual temperature increase at the outer wall. After 40 seconds of the filling process, the temperature at the outer wall remains below 23 °C, indicating effective cooling mechanisms at play. This detailed examination of the temperature distribution provides critical insights into the thermal dynamics of the cylinder during refueling, emphasizing the influence of material composition and heat transfer mechanisms.
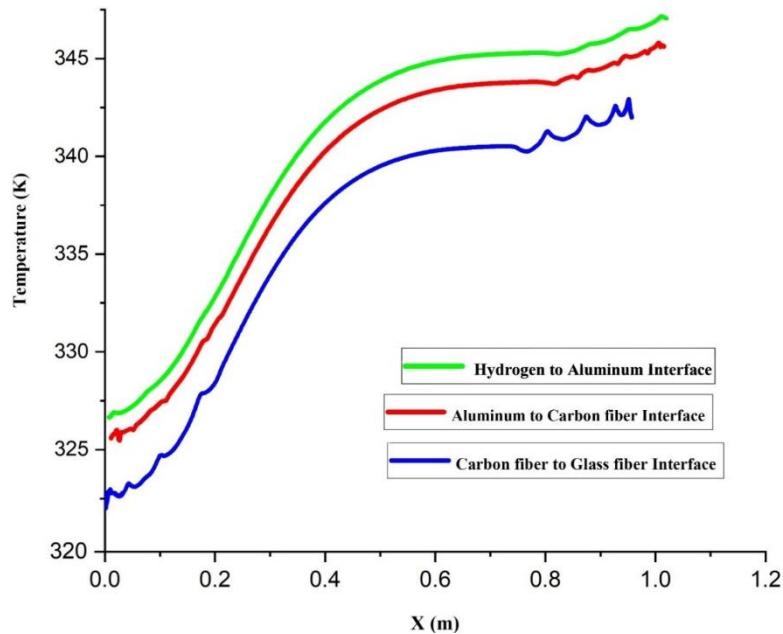

Fig. 6. Temperature distribution on each interface of Tank

Throughout the refueling process of the hydrogen cylinder, our focus centers on monitoring the temperature distribution within it. This distribution at various time intervals during refueling is visually presented in Figure 7. It is noteworthy that the gas temperature within the cylinder exhibits non-uniform characteristics, gradually increasing in both the axial and radial directions. Notably, the highest temperatures are observed in the rear or caudal region, while the lowest temperatures are closer to the inlet. The evolution of maximum temperature within the cylinder is quite interesting. It experiences rapid growth at the onset of refueling, followed by a gradual increase and eventually stabilizes towards the end of the filling process. Over the course of refueling, we observe a notable temperature increase, with the maximum temperature rising from 20°C to 80°C as the refueling time progresses from 1 seconds to 212 seconds. As the gas temperature inside the cylinder increases gradually, a significant heat transfer process occurs. Heat is transferred from the gas to the inner wall, causing the aluminum liner to experience a temperature rise. Simultaneously, a portion of the heat absorbed by the inner wall is then conducted to the carbon fiber/epoxy and further propagates into the glass fiber/epoxy. This intricate heat transfer mechanism is essential for understanding the dynamic temperature variations within the cylinder during the refueling process. Analyzing the results presented in Figure 7, it becomes evident that by the conclusion of the refueling process, the region with the maximum temperature has shifted to the bottom of cylinder. Here, the "top of the cylinder" refers to the vicinity near the cylinder's inlet, while the "bottom of the cylinder" denotes the region closer to the cylinder's base. Within cylinder, the area with the maximum temperature progressively narrows towards the cylinder's bottom as the refueling unfolds. Furthermore, our focus during the refueling process of the hydrogen vehicle cylinder is centered on monitoring the

temperature distribution within it, as depicted in Figure 7. Remarkably, the gas temperature within the cylinder exhibits non-uniform characteristics, gradually increasing both axially and radially. The highest temperatures are concentrated in the rear or caudal region, while the lowest temperatures are closer to the inlet. As the gas temperature within the cylinder steadily rises, it triggers significant heat transfer phenomena. Heat is transferred from the gas to the inner wall, resulting in a temperature increase in the aluminum liner. Simultaneously, a portion of the heat absorbed by the inner wall is further propagated to the carbon fiber/epoxy and subsequently to the glass fiber/epoxy. This intricate heat transfer process plays a pivotal role in comprehending the dynamic temperature behavior within the cylinder throughout the refueling process.
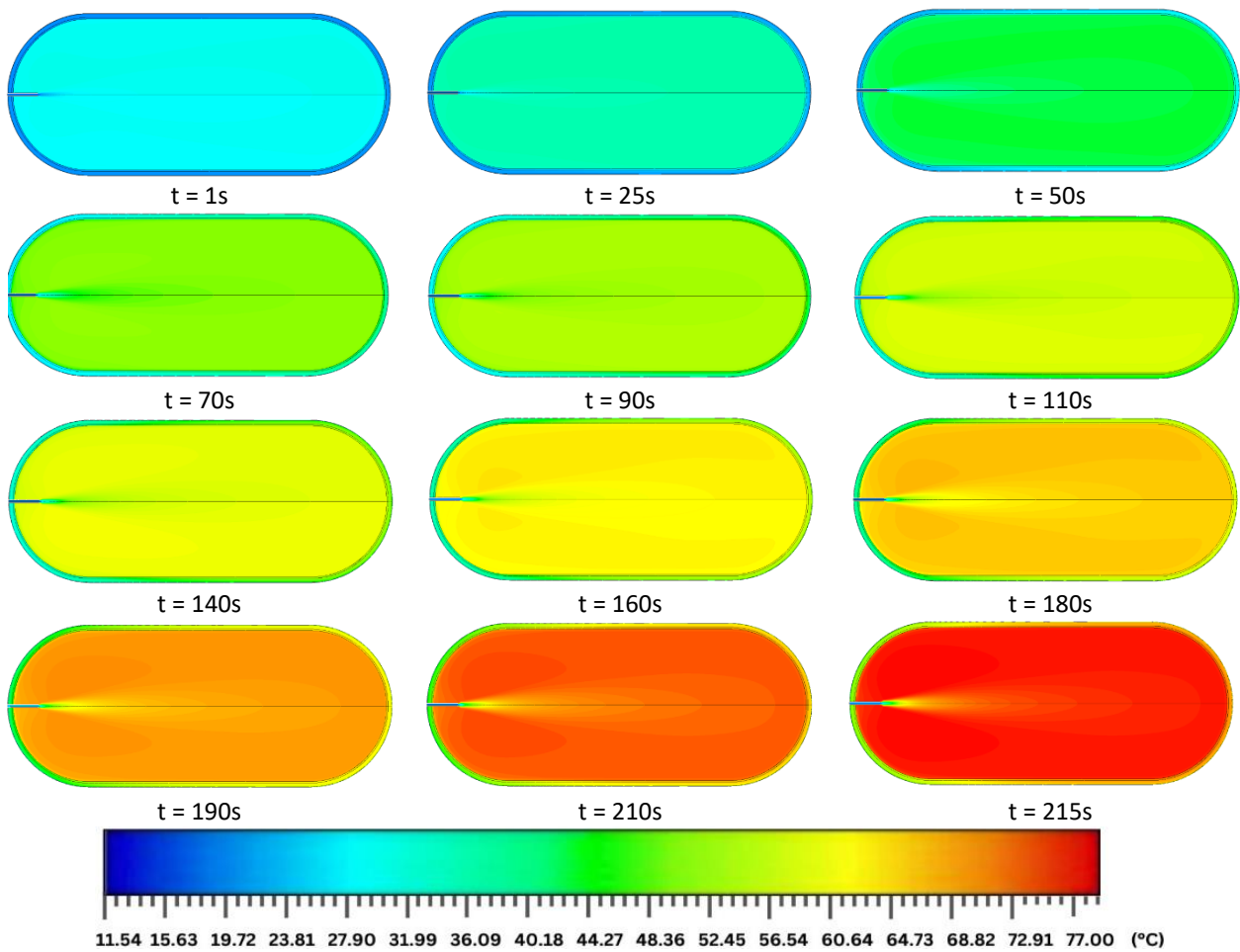

Fig. 7. Temperature distribution within cylinder

5.4 Exploring Inlet Diameter

To investigate the impact of inlet diameter, we conducted simulations using cylinders of different inlet diameters: 20 mm, 40 mm and 60 mm. The results are presented in Figure 8, which illustrates the maximum and mean temperatures during refueling for cylinders with varying inlet diameters. According to the simulation results, it can be observed that cylinders with larger inlet diameters exhibit lower maximum temperature rise compared to those with smaller diameters. Additionally, the temperature distribution is more uniform in cylinders with larger inlet diameters. This phenomenon can be attributed to the lower initial velocity of the gas in cylinders with larger inlet diameters. Opting for a smaller inlet diameter offers the advantage of better control over the maximum temperature. However, it introduces challenges in terms of manufacturing technology for

carbon fiber full-wrapped gas cylinders. Furthermore, higher gas velocity associated with smaller inlet diameters increases the likelihood of damaging the gas pipe. Therefore, when considering the inlet diameter for gas cylinders, a trade-off must be made between temperature control and manufacturing requirements, taking into account the specific needs and constraints of the system.
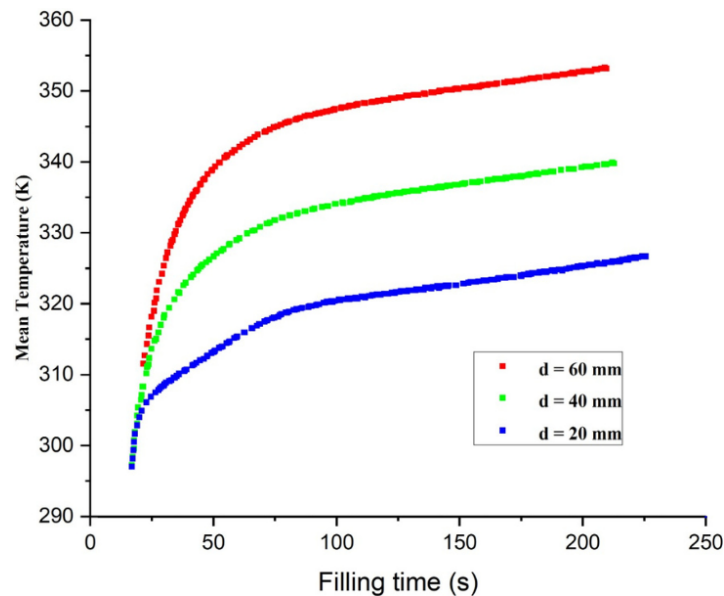

Fig. 8. Mean temperature during the refueling with different inlet diameter

5.5 Effect of Initial Pressure

We conducted a comprehensive study with a constant mass filling rate of 30 g/s, aiming to assess the impact of different initial pressures—specifically, 2, 18, and 34 MPa—on the temperature variations during the refueling process. These findings are visually depicted in Figure 8, where we observe distinct temperature trends associated with each initial pressure condition. Remarkably, when refueling commences at an initial pressure of 5 MPa, the temperature increase is most pronounced among the tested scenarios. In contrast, when the refueling process begins from an initial pressure of 34 MPa, we observe the least substantial temperature rise. This intriguing observation underscores a critical relationship between initial pressure and temperature dynamics during refueling. To elaborate further, the reason behind this phenomenon lies in the volume of hydrogen introduced into the cylinder. When refueling starts at a lower pressure, a larger quantity of hydrogen is allowed to enter the cylinder during the process. As a result, the increased mass of hydrogen undergoing compression generates more heat, leading to a more significant temperature increase. Conversely, when refueling initiates at a higher initial pressure, the volume of hydrogen introduced into the cylinder is comparatively smaller, resulting in a less pronounced temperature rise. Our investigation highlights the intricate interplay between initial pressure and temperature variations during the refueling process, shedding light on the pivotal role played by the volume of hydrogen introduced into the cylinder under different pressure conditions.

As we all know, a vehicle's fuel tank is refueled with residual fuel. Similarly, a certain amount of hydrogen gas remains in the hydrogen cylinder during refueling of the fuel cell vehicle. The pressure of the remaining gas has an impact on the maximum temperature rise during refueling. To better understand the effect of the initial pressure, fillings with initial pressures of 2, 5, 10, 15, 20, and 25 MPa were simulated when the cylinder is filled at 35 MPa with a flow rate of 40 g/s. The ambient

temperature for these fillings is 20 °C. As shown in Figure 9, the maximum temperature rise decreases as the initial pressure increases, and vice versa. A linear relationship between the initial pressure and the maximum temperature rise is revealed by Figure 9. An increase of 1 MPa in the initial pressure results in a decrease of 2.2 °C in the maximum temperature rise.
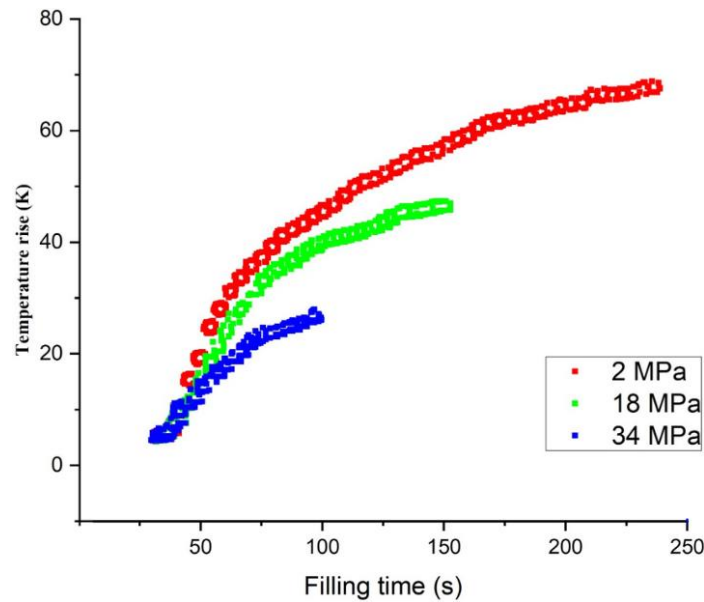
Fig. 9. Temperature rise with different initial pressure in the cylinder

## 5.6 PCM Impact on Hydrogen Tank Performance

A comparative analysis is presented between a traditional standard tank and a design incorporating phase change material (PCM). The temperature data displayed in the graphs represent the midpoint of each wall layer. In Figure 10(b), outcomes are illustrated assuming an adiabatic outer wall and no hydrogen cooling at the refueling station. The gas, initially at 16 °C, undergoes rapid heating during compression into the tank, completing the fueling process in approximately 200 s with a peak temperature reaching around 355 K. With the outer tank wall assumed to be adiabatic, heat transfer occurs solely from the gas to the surrounding walls, leading the system toward thermal equilibrium. Figure 10(b) showcases results for a standard tank, exhibiting an adiabatic temperature of approximately 80 °C and thermal equilibrium attained at 210 s. Throughout fueling, the gas thermal convection coefficient is 150 W m⁻² K⁻¹, resulting in higher heat rates for the plastic liner. Post-fueling, the convection coefficient drops to 50 W m⁻² K⁻¹, causing a sudden decrease in the liner temperature. However, the potential for hot spots exceeding 80 °C cannot be ruled out, posing a potential risk to the tank's mechanical stability.

Figure 10(a) presents temperature outcomes for the novel tank with PCM material, reaching thermal equilibrium at around 63 °C, a noteworthy 17 °C lower than the standard tank. The PCM effectively absorbs heat, maintaining the walls well below the critical temperature. However, akin to the standard case, post-fueling heat transfer affects the hydrogen temperature, necessitating considerable time to reach thermal equilibrium. A comparison with Figure 10(a) reveals a mere 2 K reduction in peak temperature with the incorporation of PCM, indicating insufficient heat transfer rates to exchange the compression heat during fueling. The hydrogen/gas interface's high thermal resistances and the suboptimal thermal properties of paraffin wax impede gas cooling, resulting in a sluggish heat transfer process. In summary, despite the presence of the PCM layer, two key

observations persist: the possibility of hot spots on the walls and consistent gas density during fueling for both tanks, resulting in an identical overall mass fueled into the storage system. Despite initial assumptions, the innovative design falls short of matching the storage performance of a regular CHG system, where hydrogen undergoes cooling before filling.

However, the comparison between standard tanks and those integrated with phase change material (PCM) reveals notable advantages and challenges. PCM-integrated tanks demonstrate lower peak temperatures, enhancing safety by reducing the risk of thermal damage and ensuring mechanical stability during refueling. This underscores the effectiveness of PCM in temperature control and safety enhancement. Furthermore, the PCM-integrated tanks achieve thermal equilibrium at lower temperatures post-fueling, signifying improved efficiency in dissipating heat and stabilizing temperatures.

Yet, challenges persist in heat transfer dynamics due to PCM's high thermal resistance, hindering effective heat exchange between hydrogen gas and PCM material. While PCM integration does not significantly alter hydrogen density or storage capacity, further research is warranted to optimize PCM selection and integration, addressing limitations in matching the storage performance of traditional compressed hydrogen gas systems. Overall, these findings emphasize the importance of balancing thermal performance, safety, and efficiency in hydrogen vehicle cylinders, highlighting the ongoing need for research and development to fully realize the potential of PCM-integrated hydrogen storage solutions.
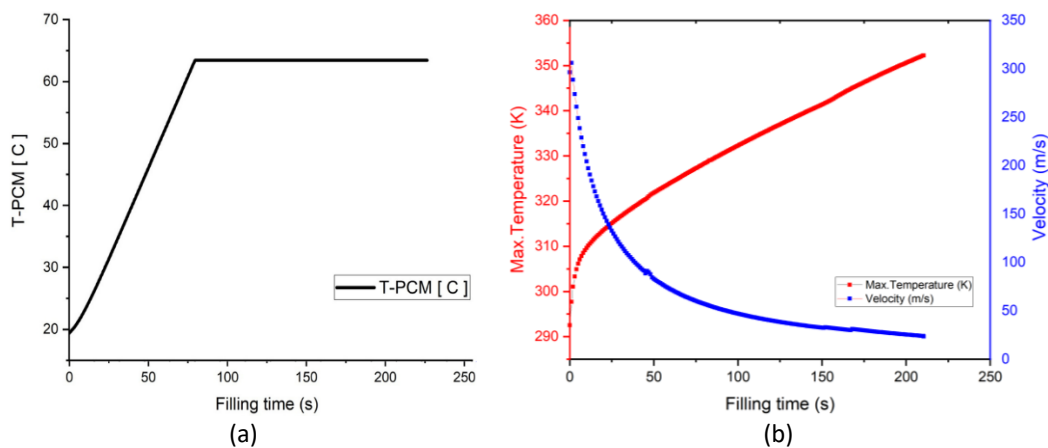
Fig. 10. (a) Temperature profiles for the two cases of tank simulated with an aluminum and PCM liner, (b) Temperature profiles aluminum liner, a carbon fiber/epoxy, and a glass fiber-epoxy

6. Conclusions

This investigation employs the Redlich-Kwong equation of real gas model to simulate the refueling process of 34 MPa, 120 L compressed hydrogen cylinders. The findings reveal that cylinders with a greater length-to-diameter ratio exhibit a more pronounced temperature increase during refueling. Specifically, the maximum temperature in cylinders with an elevated ratio manifests during the refueling process, while in smaller cylinders, it is observed towards the conclusion of refueling. Notably, refueling with an escalating mass flow rate yields lower temperatures. A Computational Fluid Dynamics (CFD) model is utilized to simulate the non-uniform temperature distribution within the cylinder, pinpointing a peak temperature in the caudal region. Comparative temperature analyses indicate that the temperature in the aluminum liner surpasses that in carbon fiber/epoxy laminates, and the latter is higher than in glass fiber/epoxy laminates. The extent of the maximum

temperature increase is contingent upon the mass flow rate, initial pressure, and ambient temperature. Specifically, there is an exponential growth concerning the mass flow rate, a reduction of 2.2 °C with a 1 MPa increase in initial pressure, and a marginal impact of ambient temperature.

To facilitate effective control, the study proposes an empirical formula for calculating the maximum temperature increase. Furthermore, it is emphasized that a full refueling process can be accomplished in less than 4 minutes when the ambient temperature remains below 310 K.

References

[1]   Zheng, Jinyang, Xianxin Liu, Ping Xu, Pengfei Liu, Yongzhi Zhao, and Jian Yang. "Development of high pressure gaseous hydrogen storage technologies." *International Journal of Hydrogen Energy* 37, no. 1 (2012): 1048-1057. https://doi.org/10.1016/j.ijhydene.2011.02.125

[2]   Babay, Mohamed-Amine, Mustapha Adar, Ahmed Chebak, and Mustapha Mabrouki. "Dynamics of Gas Generation in Porous Electrode Alkaline Electrolysis Cells: An Investigation and Optimization Using Machine Learning." *Energies* 16, no. 14 (2023): 5365. https://doi.org/10.3390/en16145365

[3]   Babay, Mohamed-Amine, Mustapha Adar, Ahmed Chebak, and Mustapha Mabrouki. "Exploring the sustainability of serpentine flow-field fuel cell, straight channel PEM fuel cells hight temperature through numerical analysis." *Energy Nexus* 14 (2024): 100283. https://doi.org/10.1016/j.nexus.2024.100283

[4]   Babay, Mohamed-Amine, Mustapha Adar, and Mustapha Mabrouki. "Modeling and Simulation of a PEMFC Using Three-Dimensional Multi-Phase Computational Fluid Dynamics Model." In *2021 9th International Renewable and Sustainable Energy Conference (IRSEC)*, pp. 1-6. IEEE, 2021. https://doi.org/10.1109/IRSEC53969.2021.9741144

[5]   Gahleitner, Gerda. "Hydrogen from renewable electricity: An international review of power-to-gas pilot plants for stationary applications." *International Journal of Hydrogen Energy* 38, no. 5 (2013): 2039-2061. https://doi.org/10.1016/j.ijhydene.2012.12.010

[6]   McManus, Marcelle C. "Environmental consequences of the use of batteries in low carbon systems: The impact of battery production." *Applied Energy* 93 (2012): 288-295. https://doi.org/10.1016/j.apenergy.2011.12.062

[7]   Garrier, S., B. Delhomme, P. De Rango, Philippe Marty, Daniel Fruchart, and Salvatore Miraglia. "A new MgH_2 tank concept using a phase-change material to store the heat of reaction." *International Journal of Hydrogen Energy* 38, no. 23 (2013): 9766-9771. https://doi.org/10.1016/j.ijhydene.2013.05.026

[8]   Liu, Yan-Lei, Yong-Zhi Zhao, Lei Zhao, Xiang Li, Hong-gang Chen, Li-Fang Zhang, Hui Zhao et al. "Experimental studies on temperature rise within a hydrogen cylinder during refueling." *International Journal of Hydrogen Energy* 35, no. 7 (2010): 2627-2632. https://doi.org/10.1016/j.ijhydene.2009.04.042

[9]   Heitsch, Matthias, Daniele Baraldi, and Pietro Moretto. "Numerical investigations on the fast filling of hydrogen tanks." *International Journal of Hydrogen Energy* 36, no. 3 (2011): 2606-2612. https://doi.org/10.1016/j.ijhydene.2010.04.134

[10]   Kim, Sung Chan, Seung Hoon Lee, and Kee Bong Yoon. "Thermal characteristics during hydrogen fueling process of type IV cylinder." *International Journal of Hydrogen Energy* 35, no. 13 (2010): 6830-6835. https://doi.org/10.1016/j.ijhydene.2010.03.130

[11]   Fuel Cell Standards Committee. *Fueling protocols for light duty gaseous hydrogen surface vehicles*. SAE International, 2010.

[12]   Mori, D., and K. Hirose. "Recent challenges of hydrogen storage technologies for fuel cell vehicles." *International Journal of Hydrogen Energy* 34, no. 10 (2009): 4569-4574. https://doi.org/10.1016/j.ijhydene.2008.07.115

[13]   Jena, Puru. "Materials for hydrogen storage: past, present, and future." *The Journal of Physical Chemistry Letters* 2, no. 3 (2011): 206-211. https://doi.org/10.1021/jz1015372

[14]   Yang, Jiann C. "A thermodynamic analysis of refueling of a hydrogen tank." *International Journal of Hydrogen Energy* 34, no. 16 (2009): 6712-6721. https://doi.org/10.1016/j.ijhydene.2009.06.015

[15]   Mohamed, Kaveh, and Marius Paraschivoiu. "Real gas simulation of hydrogen release from a high-pressure chamber." *International Journal of Hydrogen Energy* 30, no. 8 (2005): 903-912. https://doi.org/10.1016/j.ijhydene.2004.10.001

[16]   Dicken, C. J. B., and Walter Mérida. "Measured effects of filling time and initial mass on the temperature distribution within a hydrogen cylinder during refuelling." *Journal of Power Sources* 165, no. 1 (2007): 324-336. https://doi.org/10.1016/j.jpowsour.2006.11.077

[17]   Dicken, C. J. B., and Walter Mérida. "Modeling the transient temperature distribution within a hydrogen cylinder during refueling." *Numerical Heat Transfer, Part A: Applications* 53, no. 7 (2007): 685-708. https://doi.org/10.1080/10407780701634383

[18]   Pregassame, Sitra, Frédéric Barth, L. Allidieres, and K. Barral. "Hydrogen refuelling station: filling control protocols

development." In *Proceedings of the Sixteenth World Hydrogen Energy Conference*, pp. 13-16. 2006.

[19] Maus, Steffen, Jobst Hapke, Chakkrit Na Ranong, Erwin Wüchner, Gerardo Friedlmeier, and David Wenger. "Filling procedure for vehicles with compressed hydrogen tanks." *International Journal of Hydrogen Energy* 33, no. 17 (2008): 4612-4621. https://doi.org/10.1016/j.ijhydene.2008.06.052

[20] Ramasamy, Vishagen, Edward S. Richardson, Philippa Reed, Warren Hepples, and Andrew Wheeler. "Investigating the use of phase-change materials for temperature control during fast filling of hydrogen cylinders." *High Temperature Material Processes: An International Quarterly of High-Technology Plasma Processes* 22, no. 2-3 (2018). https://doi.org/10.1615/HighTempMatProc.2018024731

[21] Melideo, Daniele, Daniele Baraldi, N. De Miguel Echevarria, and B. Acosta Iborra. "Effects of some key-parameters on the thermal stratification in hydrogen tanks during the filling process." *International Journal of Hydrogen Energy* 44, no. 26 (2019): 13569-13582. https://doi.org/10.1016/j.ijhydene.2019.03.187

[22] Rothuizen, E., W. Mérida, Masoud Rokni, and M. Wistoft-Ibsen. "Optimization of hydrogen vehicle refueling via dynamic simulation." *International Journal of Hydrogen Energy* 38, no. 11 (2013): 4221-4231. https://doi.org/10.1016/j.ijhydene.2013.01.161

[23] Zhao, Lei, Quanliang Zhao, Jie Zhang, Shuo Zhang, Guangping He, Mengying Zhang, Tingting Su, Xu Liang, Can Huang, and Wenhui Yan. "Review on studies of the emptying process of compressed hydrogen tanks." *International Journal of Hydrogen Energy* 46, no. 43 (2021): 22554-22573. https://doi.org/10.1016/j.ijhydene.2021.04.101

[24] Liszka, Miroslaw, Aleksandr Fridlyand, Ambalavanan Jayaraman, Michael Bonnema, and Chakravarthy Sishtla. "Hydrogen Fast Fill Modeling and Optimization of Cylinders Lined With Phase Change Material." In *ASME International Mechanical Engineering Congress and Exposition*, vol. 84584, p. V010T10A052. American Society of Mechanical Engineers, 2020. https://doi.org/10.1115/IMECE2020-24154

[25] Rahim, Nasrullah Che, Muhammad Fairuz Remeli, Baljit Singh, and Hazim Moria. "Designing a Solar Heat Storage System using Heat Pipe and Phase-Change Material (PCM)." *Journal of Advanced Research in Fluid Mechanics and Thermal Sciences* 91, no. 1 (2022): 102-114. https://doi.org/10.37934/arfmts.91.1.102114

[26] Farid, Mohammed M., Amar M. Khudhair, Siddique Ali K. Razack, and Said Al-Hallaj. "A review on phase change energy storage: materials and applications." *Energy Conversion and Management* 45, no. 9-10 (2004): 1597-1615. https://doi.org/10.1016/j.enconman.2003.09.015

[27] Dincer, Ibrahim. "On thermal energy storage systems and applications in buildings." *Energy and Buildings* 34, no. 4 (2002): 377-388. https://doi.org/10.1016/S0378-7788(01)00126-8

[28] Lane, George A. "Low temperature heat storage with phase change materials." *International Journal of Ambient Energy* 1, no. 3 (1980): 155-168. https://doi.org/10.1080/01430750.1980.9675731

[29] Abhat, A. "Low temperature latent heat thermal energy storage: heat storage materials." *Solar Energy* 30, no. 4 (1983): 313-332. https://doi.org/10.1016/0038-092X(83)90186-X

[30] Zhao, Lei, Yanlei Liu, Jian Yang, Yongzhi Zhao, Jinyang Zheng, Haiyan Bie, and Xianxin Liu. "Numerical simulation of temperature rise within hydrogen vehicle cylinder during refueling." *International Journal of Hydrogen Energy* 35, no. 15 (2010): 8092-8100. https://doi.org/10.1016/j.ijhydene.2010.01.027

[31] Yang, Jiann C. "A thermodynamic analysis of refueling of a hydrogen tank." *International Journal of Hydrogen Energy* 34, no. 16 (2009): 6712-6721. https://doi.org/10.1016/j.ijhydene.2009.06.015